CTOL Ski Jump: Analysis, Simulation, and Flight Test

John W. Clark Jr.* and Marvin M. Walters†
Naval Air Development Center, Warminster, Pennsylvania

In the past several years, the ski-jump (ramp-assisted) launch concept has received considerable attention within the U.S. Navy. The specific goal was set (and achieved) to demonstrate through flight test the feasibility of, and quantify performance gains from, ski-jump launch of the T-2C, F-14A, and F/A-18A aircraft using a 100-ft ramp with variable end angles of 6 and 9 degs. The analysis, piloted simulation, performance predictions, and flight safety considerations leading to flight test, as well as a comparison of analytical predictions with flight test results for the three aircraft, are discussed. The developed analytical capability, although somewhat conservative, proved to be highly effective in preparation for, and support of, the flight test and in successfully predicting the 40-60% reduction in takeoff distance demonstration in flight test.

Nomenclature

a_x, a_z	= body axis accelerations, g (positive forward and down)
F_A	= strut air shock force, lb
F_D	= hydraulic damping force, lb
F_f, F_N	= tire friction and normal forces, respectively, lb
F_s	= strut axial load, lb
F_{s_p}	= pilot stick force, lb (positive push)
F_{t_n}, F_{t_s}	= tire loads in strut axes, lb
g	= acceleration of gravity, ft/s^2
I_y	= aircraft inertia, slugs-ft^2
K_D	= hydraulic damping factor, lb/in.^{2}/s^2
$K_{\theta_e}, K_\theta, K_{\int\theta}$	= pilot model feedback gains, lb/deg, lb/deg/s, lb/deg-s, respectively
m	= aircraft mass, slugs
m_u	= landing gear unsprung mass, slugs
M	= pitch moment, ft-lb (positive nose-up)
q	= body axis pitch rate, deg/s (positive nose-up)
R	= ramp radius of curvature, ft
s	= landing strut stroke, in., or Laplace variable
u, w	= body axis velocities, ft/s (positive forward and down)
V	= total velocity, ft/s
x, z	= body axis coordinates, ft (position forward and down)
X, Z	= body axis forces, lb (positive forward and down)
θ	= pitch angle, deg (positive nose-up)
θ_e	= pilot model pitch error, deg
θ_r	= local ramp angle, deg
θ_s	= landing gear strut inclination, deg
μ	= rolling coefficient of friction

Subscripts

A/C	= aircraft axis reference
c	= commanded quantity
0	= initial value
ax	= referenced to landing gear axle

Acronyms

GAC	= Grumman Aircraft Co.
McAir	= McDonnell Aircraft Co.
NADC	= Naval Air Development Center
NASA	= NASA Ames Research Center
NTEC	= Naval Training Equipment Center

Introduction

THE ramp-assisted takeoff (ski-jump) concept provides the potential for a passive means of launching aircraft from a confined operational area (ship or short runway) without the need for catapult boost equipment. The past five years have seen considerable effort on the part of the U.S. Navy to verify quantitatively the feasibility of ski jump as a viable means of reducing the required takeoff ground roll for naval conventional takeoff and landing (CTOL) aircraft. This paper will overview the complete development effort: analysis, manned simulation, and correlation with subsequent flight test results.

The ski-jump concept uses a ramp to rotate the aircraft flight path from horizontal to a positive climb angle at forward speed less than that normally required to rotate the aircraft aerodynamically. This early rotation and lift-off provides an initial rate-of-climb and altitude margin that allows the aircraft to accelerate to flying speed while in a partial ballistic trajectory. Reduction in takeoff distance is achieved primarily as a result of liftoff speeds that may be considerably below the stall speed of the aircraft (see Fig. 1). The reader is referred to Ref. 1 for a more detailed description of the segments of a ski-jump trajectory in comparison with a conventional takeoff.

Beginning with an initial, abbreviated (15-takeoff) flight test demonstration using the T-2C in October 1980,[2] the ski-jump program has progressed systematically through detailed analysis, piloted flight simulation, and extensive flight test (Fig. 2) of the T-2C, F-14A, F/A-18A, and S-3A.

This paper details the salient points of the analysis, simulations, and flight tests. A description of the analytical and simulation models is presented along with an outline of the flight test setup and procedures. The aircraft configurations and flight conditions tested are also summarized, with a comparison of the predicted and flight test results presented for these conditions.

Analysis and Simulation

Prior to initiation of flight test, the ski-jump characteristics (structural integrity, stability, controllability, and performance) of each aircraft were analyzed. First, the aircraft performance, control, and loads were predicted for the anticipated ranges of aircraft configurations and flight condi-

Received April 11, 1985; revision received Dec. 12, 1985.

*Senior Aerospace Engineer, Flight Dynamics, Aircraft and Crew Systems Technology Directorate. Member AIAA.

†Senior Aerospace Engineer, Aerodynamics, Aircraft and Crew Systems Technology Directorate. Member AIAA.

tions using a three-degree-of-freedom (longitudinal, vertical, and pitch rotation) nonreal time analysis. At least one, and in most cases more than one, piloted flight simulation(s) served as pilot training and validation of the three-degree-of-freedom results. These piloted simulations also provided a means to assess crosswind effects, develop pilot control techniques, and determine safety of flight limits (e.g., single-engine control and crew ejection envelopes).

Three-Degree-of-Freedom Analysis

The model developed for the initial ski-jump analysis was limited to the three longitudinal degrees of freedom in order to keep it tractable and relatively inexpensive while still providing information on the essential parameters of the problem (performance, control, and landing-gear structural loads). Equations (1-8) define the trajectory dynamics.

$$\dot{u} = X/m - qw - g\sin\theta \tag{1}$$

$$\dot{w} = Z/m + qu + g\cos\theta \tag{2}$$

$$\dot{q} = M/I_y \tag{3}$$

$$\dot{\theta} = q \tag{4}$$

$$a_x = (\dot{u} + qw)/g \tag{5}$$

$$a_z = (\dot{w} - qu)/g \tag{6}$$

$$\dot{x} = u\cos\theta + w\sin\theta \tag{7}$$

$$\dot{Z} = -u\sin\theta + w\cos\theta \tag{8}$$

The model was partitioned into a number of discrete subelements (Fig. 3), including nonlinear aerodynamic and thrust forces and moments, nonlinear landing-gear strut load, and damping characteristics and control system dynamics. Additionally, a model for pilot control strategy was included to provide the capability to analyze pilot-in-the loop pitch control.

The applied aerodynamic forces and moments were assumed to be nonlinear functions of angle of attack, stabilizer deflection, flap deflection, and height above ground, and the aircraft net thrust was modeled as a function of velocity, throttle setting, and ambient air temperature.

The aircraft landing gear (both nose and main gear) was assumed to consist of unidirectional spring/damper struts rigidly attached to the aircraft structure at one end and the wheel/tire assembly at the other. Motion of the landing gear relative to the airframe is defined by differential dynamic equations, which describe the acceleration, velocity, and displacement of the "unsprung mass" (m_u), i.e., wheel, tire,

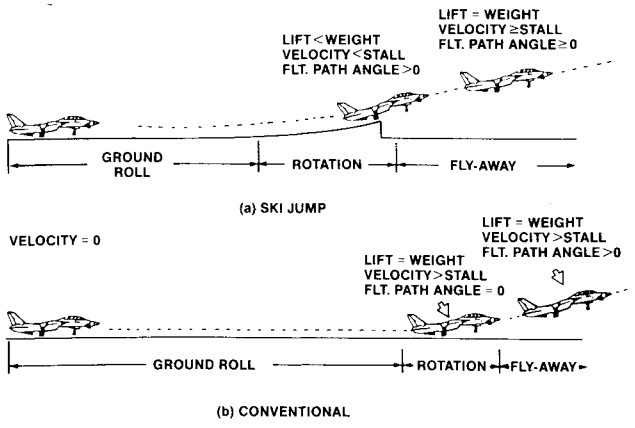

Fig. 1 Takeoff trajectory segments.

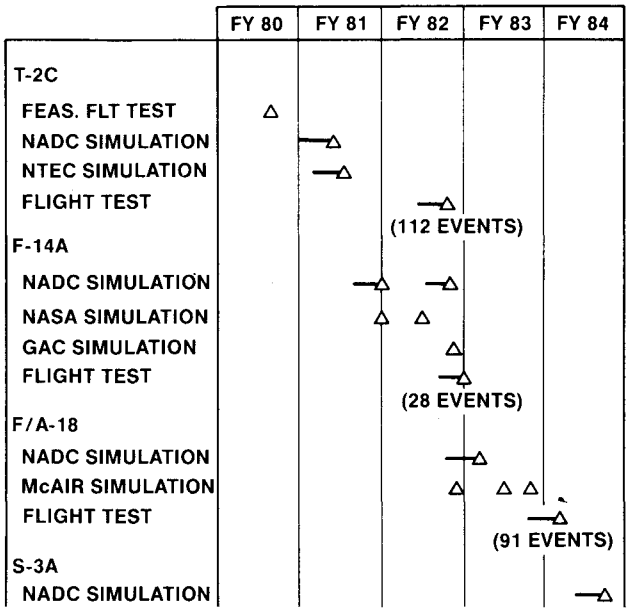

Fig. 2 Navy ski-jump program.

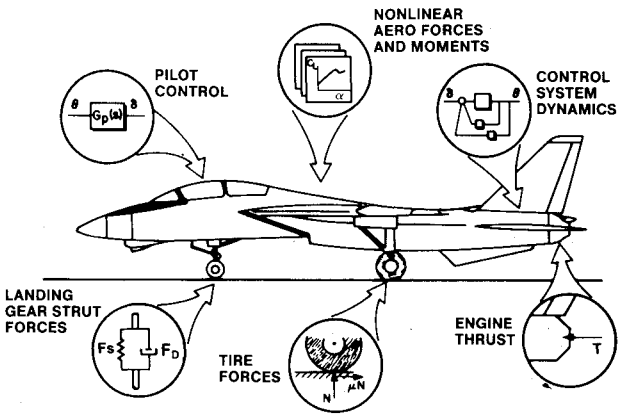

Fig. 3 Ski-jump analysis model components.

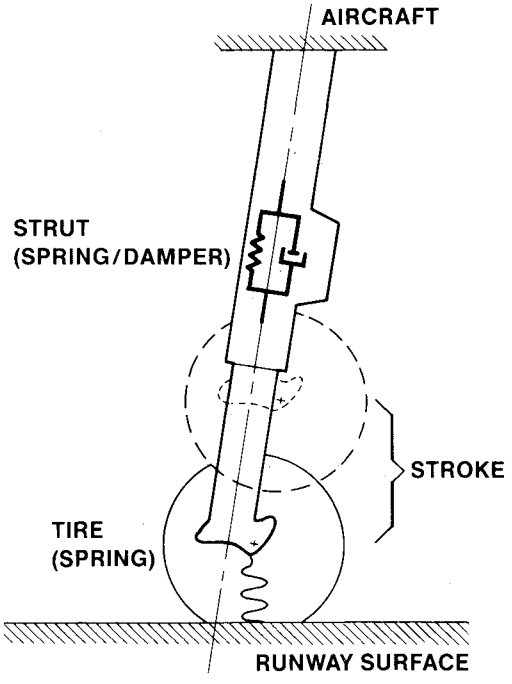

Fig. 4 Landing gear schematic.

and moving portion of the shock strut. External forces acting on the unsprung mass include nonlinear spring and damping force due to shock strut compression and nonlinear, undamped spring force due to tire compression. Figure 4 provides a schematic representation of a typical landing gear with Fig. 5 showing the external forces assumed to act on the system. The strut force F_s consists of an airspring force F_A, which is a function of the stroke and a hydraulic damping force F_D, which is typically expressed as a damping factor ($K_D = F_D/\dot{s}^2$), which is also a function of the stroke.

$$F_s = F_A + K_D \dot{s}^2 \tag{9}$$

The tire normal force F_N is defined by a nonlinear function of tire compression Δr and the tangential force F_f is given by

$$F_f = \mu F_N (\dot{x}/|\dot{x}|) \tag{10}$$

The value used for μ, the rolling friction coefficient, is 0.015. Resolving the tire forces into the strut axis system yields

$$F_{t_s} = F_N \cos(\theta_s + \theta - \theta_r) + F_f \sin(\theta_s + \theta - \theta_r) \tag{11}$$

$$F_{t_n} = -F_N \sin(\theta_s + \theta - \theta_r) + F_f \cos(\theta_s + \theta - \theta_r) \tag{12}$$

The differential equations defining the stroke dynamics are

$$\ddot{s} = (F_{t_s} - F_s)/m_u - g\cos(\theta_s + \theta) - \ddot{\zeta} \tag{13}$$

$$\dot{s} = \dot{s}_o + \int \ddot{s}\,dt \tag{14}$$

$$s = s_o + \int \dot{s}\,dt \tag{15}$$

where $\ddot{\zeta}$ is the acceleration of the fully compressed axle location (x_{ax}, z_{ax} relative to the aircraft c.g.) in the strut reference frame and is defined in terms of aircraft dynamics by Eq. (16):

$$\ddot{\zeta} = (\dot{u} + z_{ax}\dot{q} - x_{ax}q^2)\sin\theta_s + (\dot{w} - x_{ax}\dot{q} - z_{ax}q^2)\cos\theta_s \tag{16}$$

The landing gear induced forces and moment acting on the aircraft consist of the strut force F_s and the total tire force normal to the strut F_{t_n}.

Pitch control and stability augmentation and control force characteristics were modeled for each aircraft. In order to allow for limited pilot-in-the loop analysis, a mathematical pilot control model was also developed. The model determines appropriate control force inputs in response to pitch attitude command as depicted in Fig. 6. The allowable attitude command structure is shown in the upper half of the figure. Two discrete attitude commands are provided at two points determined spatially along the aircraft trajectory. In order to smooth the transition from one command to another, the command is ramped in over a distance that approximates 0.2-s trajectory time (i.e., $\Delta x = 0.2\dot{x}$).

The commanded attitude, once determined, drives the pilot control model shown at the bottom of Fig. 6 and described by Eqs. (17-20):

$$\theta_e = \theta_c - \theta \tag{17}$$

$$F_{s_{p_c}} = -K_{\theta_e}\theta_e - K_{\int\theta}\int \theta_e dt + K_{\dot{\theta}}\dot{\theta} \tag{18a}$$

$$\left|\int \theta_e dt\right| \le 1 \text{deg-s} \tag{18b}$$

$$\dot{F}_{s_p} = 1/0.2(F_{s_{p_c}} - F_{s_p}) \tag{19a}$$

$$\left|\dot{F}_{s_p}\right| \le 60 \text{ lb/s} \tag{19b}$$

$$F_{s_p} = \int \dot{F}_{s_p} dt \tag{20}$$

The model attempts to pitch the aircraft to the commanded attitude, nulling the error. Damping is provided through the inclusion of an attitude rate feedback, and a limited integral of attitude error is fed back to the control to reduce the effects of off-nominal trim and changing trim characteristics with speed. The stick force rate is limited to smooth the initial command transient. A first-order lag of 0.2 s is included to approximate the pilot input.

Where applicable flight or simulator data are available, they may be used to determine the values for the pilot gains: $K_{\theta_e}, K_{\dot{\theta}}, K_{\int\theta}$. Values for the pilot gains used in this analysis are approximately in the ratio of 3:2:1 with the attitude gain ranging from 2-6 lb/deg. These gains must be tailored to the specific control force gradient and response of the aircraft being analyzed.

A digital computer program was developed to implement the model. Results obtained from the three-degree-of-freedom

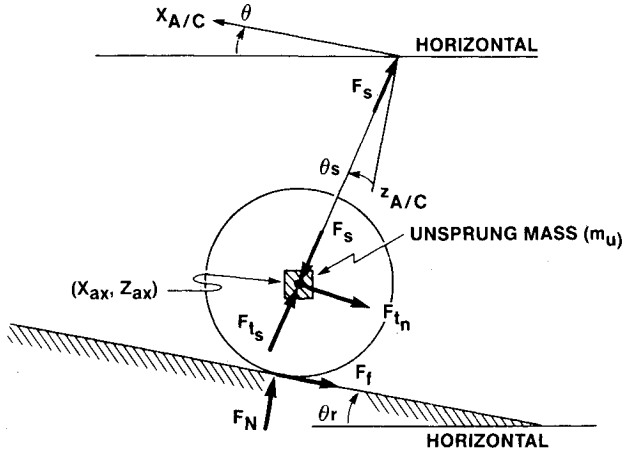

Fig. 5 Landing gear force diagram.

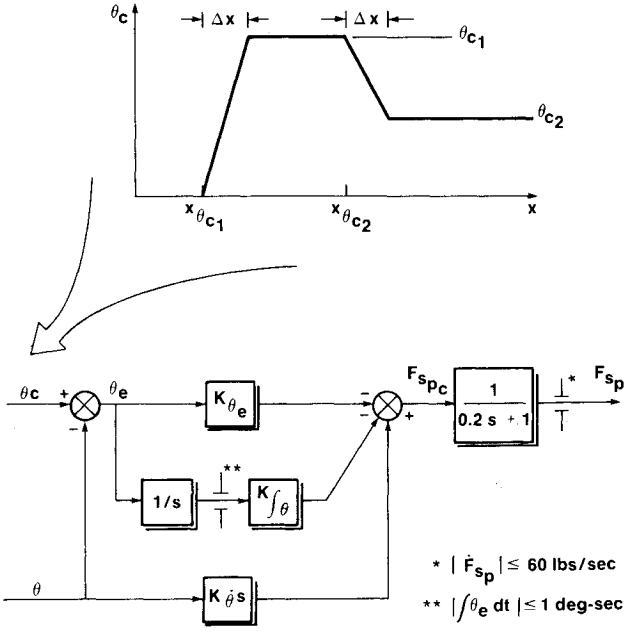

Fig. 6 Pitch control pilot model.

analyses are presented in the results section and were used to define the parameter variations and scope of the piloted real-time flight simulations.

Six-Degree-of-Freedom Piloted Simulation

While the three-degree-of-freedom performance and control results (both with and without the pilot-in-the-loop) were very promising, manned simulation was deemed necessary before a flight test demonstration could be initiated. Questions regarding pilot technique and lateral/directional control had to be answered. No less important was the need to familiarize pilots with the unique flight characteristics of ski-jump takeoffs.

Six-degree-of-freedom pilot-in-the-loop simulations were conducted for the T-2C, F-14A, and F/A-18A aircraft. The T-2C was simulated at the Naval Training Equipment Center (NTEC), the F-14A on the Flight Simulator for Advanced Aircraft at the NASA Ames Research Center, and the F/A-18A on the Manned Aircraft Combat Simulator (MACS 3.5) at McDonnell Aircraft (MCAIR), St. Louis. Math models used for all simulations consisted of flight validated aircraft models modified to include landing-gear dynamics and ski-jump ramp geometries. The simulations included both hands-off and piloted takeoffs, crosswind and headwind conditions, and both engine and system failure simulations. The results of these simulations were used to validate the analytical results, to scope the flight test program, and to substantiate pretest flight safety certification requests.

Flight Test

Test Equipment

The ski-jump flight tests were conducted at the Naval Air Test Center (NATC), Patuxent River, Maryland. A 2000-ft-long, 60-ft-wide extension to an existing runway was constructed of AM-2 matting.[3] Additional AM-2 matting was placed on the right-hand side of the runway to permit taxiing around the ramp and onto the existing runway. This runway led to the variable-exit-angle ski jump, which was designed and erected by the Naval Air Engineering Center. The ramp is 60 ft wide and 112.1 ft long for the three- and six-degree configurations, and 122.1 ft for the nine-degree configuration. The ramp is constructed of steel, consisting of an initial fixed-angle section 42 ft long followed by 10×30 ft modules mounted on steel pedestals. As shown in Fig. 7 (Ref. 4), the height of these pedestals is variable to provide the desired curvature, which was an approximate circular arc, with the ramp exit angle determined by the angle of the last inclined section. The final module was horizontal to allow the landing gear to unload prior to leaving the ramp. A modified hold-back/release was developed to assist the F-14 and F-18 in maintaining aircraft position at any location on the runway while the engines stabilized at the desired power setting before commencement of the ground run.

Table 1 Aircraft configuration summary

Airplane	Takeoff configuration	Gross weight, lb	Thrust/weight
T-2C	Half flaps (16 deg) and	10,000	0.50
	Full flaps (33 deg)	11,800	0.42
F-14A	Full flaps	48,000	0.42 (MIL)[a]
	(35 deg)	55,000	0.36 (MIL)
F/A-18A	Half flaps	32,800	0.51 (MIL)
			0.76 (MAX A/B)[b]
	(30 deg)	37,000	0.46 (MIL)
			0.67 (MAX A/B)

[a]MIL = military thrust. [b]MAX A/B = maximum afterburner.

Test Aircraft

Three aircraft were used during the test program: a T-2C, F-14A, and F/A-18A (Fig. 8). All were production-configured airplanes with the exception of airborne telemetry/magnetic tape instrumentaton and landing gear-instrumentation installed for data collection and reflectors mounted on the vertical fin for tracking data during ground acceleration run and takeoff. All tests were conducted with the aircraft in normal takeoff configuration with the gross weights and flap settings summarized in Table 1.

Test Procedure

Before the actual ski-jump operations for each airplane, a series of ground tests were conducted to establish performance and safety criteria. Ground roll acceleration tests were conducted to relate airplane ground roll to airplane thrust, gross weight, and flap configuration. These data were used during the ski-jump takeoffs in positioning the airplane behind the ramp to achieve a desired ramp end speed. In addition, simulated single-engine takeoff ground roll tests were conducted to define "abort-capable"/"committed-to-takeoff" velocity limits, providing the pilot with velocity cues in the event of an engine failure during the takeoff ground roll.

Criteria for establishing the minimum takeoff airspeed during the ski-jump tests comprised two limiting factors: 1) reaching limit angle of attack and 2) reaching zero minimum rate of climb. The initial ski-jump takeoff airspeed for each aircraft gross weight, thrust setting, and flap configuration was as close as possible to normal takeoff airspeed within any structural loading limitations predicted for the high-speed/high-ramp-angle conditions. Successive takeoff conditions were then determined by a 3- to 5-knot decrease in airspeed until one of the above criteria was reached. Each takeoff was conducted according to the following procedure:

1) Select ramp end speed and set longitudinal trim to provide the desired rotation.

2) Calculate ramp exit true airspeed, ground speed, and installed gross thrust according to local environmental conditions.

3) Position the airplane at the resulting desired takeoff ground roll start position.

4) Upon landing, refuel airplane for next test run.

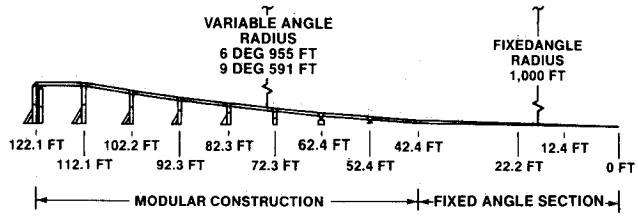

Distance along ramp, ft	Height, ft	
	6 deg exit angle	9 deg exit angle
0	0	0
12.4	0.19	0.19
22.2	0.41	0.41
42.4	1.16	1.16
52.4	1.68	1.71
62.4	2.30	2.44
72.3	3.03	3.33
82.3	3.88	4.40
92.3	4.81	5.62
102.2	5.85	7.02
112.1	5.85	8.58
122.1	—	8.58

Fig. 7 Ski-jump profile drawing.

Table 2 Ski-jump flight test summary

Aircraft	Ramp angle, deg	Gross weight, lb	Configuration	No. of events	Ground roll Minimum, ft	Ground roll Maximum, ft	Ramp speed Minimum, knots	Ramp speed Maximum, knots	Ramp exit airspeed Minimum, KEAS	Ramp exit airspeed Maximum, KEAS
T-2C	6	10,000	Half flaps	14	550	925	72	93	78	93
			Full flaps	9	425	800	63	87	70	87
		11,800	Half flaps	8	975	1,300	88	100	86	99
			Full flaps	12	625	1,175	70	97	76	91
		Various (pilot fam)	Half flaps	19	610	1,025	76	93	82	95
			Full flaps	1	1,025	—	93	—	91	—
	9	10,000	Half flaps	13	435	860	65	90	72	90
			Full flaps	14	375	700	59	82	64	79
		11,800	Half flaps	7	875	1,150	83	96	85	90
			Full flaps	9	625	1,050	72	91	71	94
		Various (pilot fam)	Half flaps	6	675	900	80	90	76	91
F-14A	6	48,000	MIL	10	1,350	1,750	106	120	101	115
		55,000	thrust	8	1,625	1,960	108	122	101	120
	9	48,000	MIL	5	1,250	1,525	104	114	103	117
		55,000	thrust	5	1,550	2,025	108	124	106	124
F/A-18A	6	32,800	MIL	15	1,075	1,475	105	122	102	123
		37,000	thrust	13	1,400	1,775	111	125	110	125
		32,800	MAX A/B	9	640	900	97	117	98	115
		37,000	thrust	14	690	1,100	95	121	99	116
	9	32,800	MIL	10	850	1,375	95	120	98	122
		37,000	thrust	11	1,250	1,575	106	118	106	121
		32,800	MAX A/B	9	385	650	81	103	82	109
		37,000	thrust	10	575	950	93	116	90	117

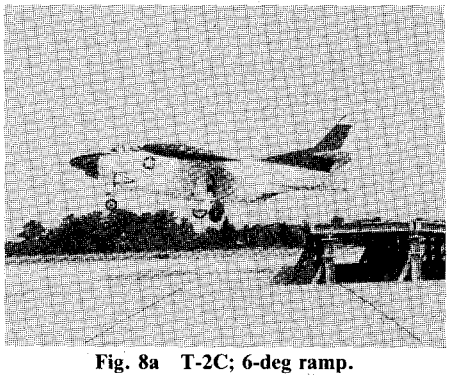

Fig. 8a T-2C; 6-deg ramp.

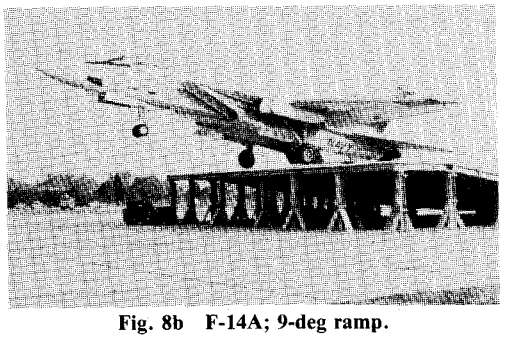

Fig. 8b F-14A; 9-deg ramp.

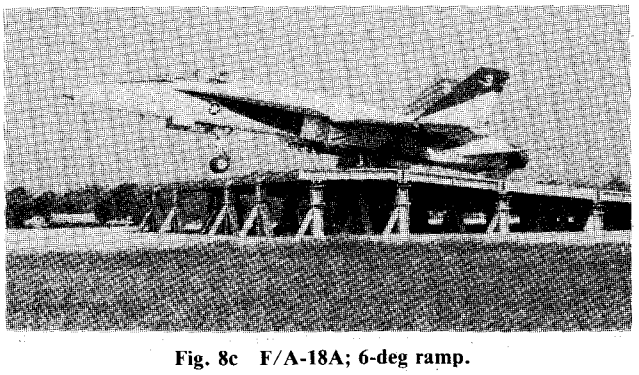

Fig. 8c F/A-18A; 6-deg ramp.

Test Conditions

The various aircraft gross weight/configuration conditions tested as part of the flight test program are summarized for the six- and nine-degree ramps in Table 2 (Ref. 4).

The minimum distances tabulated for ground roll are indicative of the takeoff performance that can be expected with the use of a ski jump, with the exception of those tabulated for the F-14A. The minimum airspeeds tested for the F-14A were restricted to 100 knots for safety considerations in the event of an engine failure during takeoff. These same restrictions precluded any takeoff with afterburner.

Results

The results of the ski-jump program, defining the minimum takeoff airspeed to achieve zero rate of climb, are typified by Figs. 9 and 10 for the F/A-18A. These figures contain the variation of minimum rate of climb with ramp end airspeed predicted by the three-degree-of-freedom analysis in comparison with the flight test results for both the 32,800 and 37,000 lb gross weights using the 9-deg ramp. The two curves on each graph represent the variation in takeoff performance with and without the pilot model "in-the-loop." The *pitch capture* represents a takeoff in which the pilot model atempts to maintain a prescribed pitch attitude after the aircraft clears the ramp (e.g., for the F/A-18A the prescribed attitude was 15 deg). The stick-free curve represents hands-off performance with no pilot input until after the aircraft trajectory has stabilized. The trends indicated by the flight test data are accurately repeated by the analytical results, with good correlation indicated between the two sets of data.

Figure 11 presents typical results of three-degree-of-freedom analysis predictions of aircraft nose and main landing-gear axle loads in comparison with the flight test results again for the F/A-18A using the 9-deg ramp. The data presented for the main gear loads represent an average of the right and left gear loads. Again, the trends established by the flight test data are duplicated by the analytical results with good correlation limited to only certain speed ranges for both the nose and main gear. Both gear loads, however, are well under the limit loads of 78,000 lb for the nose gear and 75,000 lb for each of the main gear. A similar comparison for the

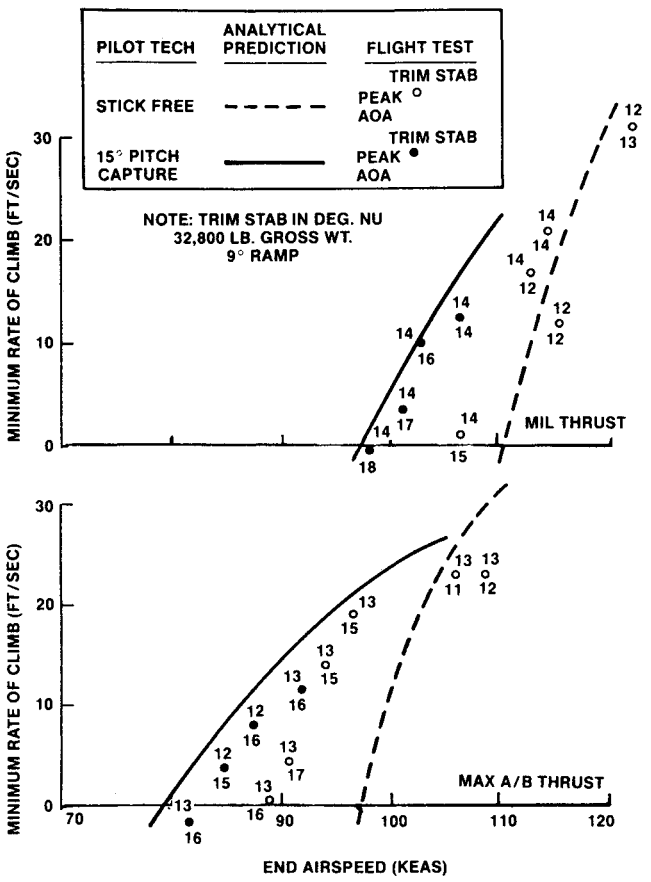

Fig. 9 F/A-18A ski-jump minimum rate of climb (prediction vs flight test).

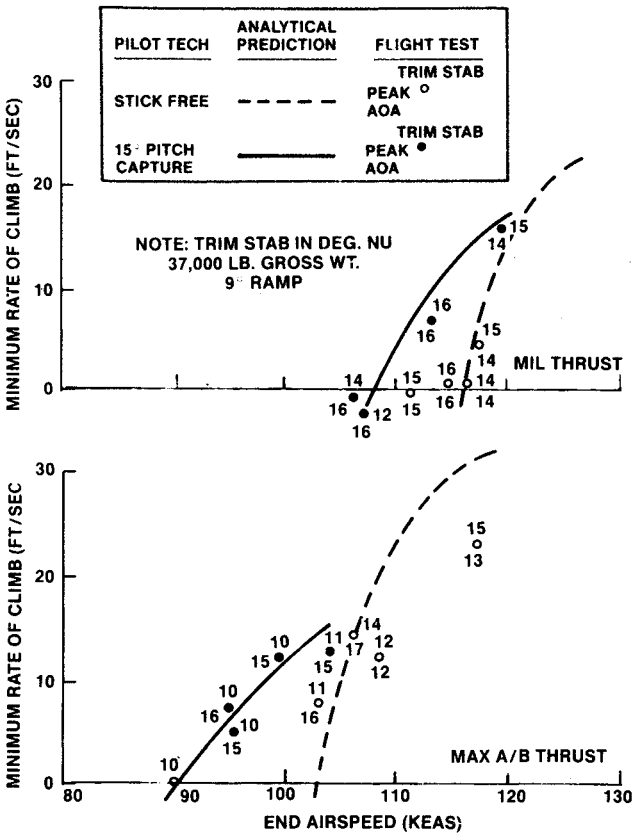

Fig. 10 F/A-18A ski-jump minimum rate of climb (prediction vs flight test).

Table 3 Summary of predicted minimum takeoff airspeed compared to flight test results

			Minimum[a] takeoff airspeed, KEAS	
			6-deg ramp	9-deg ramp
Airplane	Flaps or thrust	Gross weight, lb	Flight test/ prediction	Flight test/ prediction
T-2C	Half flaps	10,000	78/80	72/73
		11,800	86/87	85/88
	Full flaps	10,000	70/70	64/66
		11,800	76/79	78/78
F-14A[b]	MIL	48,000	101/99	103/89
	Full flaps	55,000	101/108	106/94
F/A-18A	MIL	32,800	102/102	98/97
	Half flaps	37,000	110/110	106/107
	MAX A/B	32,800	92/90	82/79
	Half flaps	37,000	99/99	90/91

[a]Minimum speed as defined by zero rate of climb. [b]Minimum speed limited to 100 knots due to single-engine safety.

F-14A and T-2C aircraft also indicated the ski-jump gear loads to be well within the respective limit loads. Note that the loads were found to be predominantly dependent on end speed and independent of thrust level.

An interesting result of the ski-jump data analysis is presented in Fig. 12, again for the F/A-18A but representative of the F-14A and T-2C as well. This figure contains the variation of aircraft maximum normal acceleration flight test data with ramp end ground speed in comparison with prediction. Also shown is the theoretical centrifugal acceleration calculated for a circular arc of the same radius as the ski-jump ramp. Aside from the good correlation between simulation and flight test data, the interesting aspect of these data is the

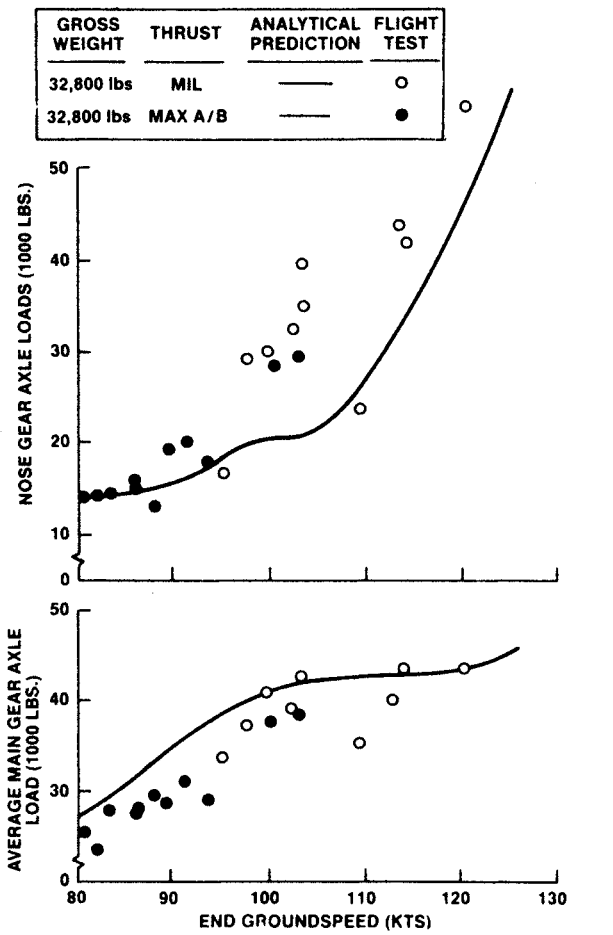

Fig. 11 F/A-18A ski-jump maximum gear loads on 9-deg ramp (prediction vs flight test).

Table 4 Ski-jump performance summary

Airplane	Flaps or thrust	Gross weight, lb	Minimum[a] takeoff airspeed, KEAS 6-deg ramp	Minimum[a] takeoff airspeed, KEAS 9-deg ramp	Field takeoff airspeed, KEAS	Minimum[a] ground roll, ft 6-deg ramp	Minimum[a] ground roll, ft 9-deg ramp	Field takeoff distance, ft
T-2C	Half flaps	10,000	78	72	93	600	450	930
		11,800	86	85	101	975	875	1320
	Full flaps	10,000	70	64	88	425	375	850
		11,800	76	78	95	625	625	1170
F-14A[b]	MIL	48,000	101	103	125	1350	1250	1800
	Full flaps	55,000	101	106	127	1700	1550	2050
F/A-18A	MIL	32,800	102	98	146	1075	850	1930
	Half flaps	37,000	110	106	154	1400	1250	2740
	MAX A/B	32,800	92	82	146	580	385	1140
	Half flaps	37,000	99	90	154	700	575	1740

[a]Minimum speed and ground roll as defined by zero rate of climb. [b]Minimum speed limited to 100 knots due to single engine safety consideration.

Table 5 CTOL ski-jump comparison of reduction in takeoff distance

Airplane	Flaps or thrust	Gross weight, lb	Reduction in takeoff ground roll, % 6-deg ramp	Reduction in takeoff ground roll, % 9-deg ramp	Reduction in distance over a 50-ft obstacle, % Maximum 6-deg ramp	Reduction in distance over a 50-ft obstacle, % Maximum 9-deg ramp	Corresponding takeoff airspeeds, KEAS 6-deg ramp	Corresponding takeoff airspeeds, KEAS 9-deg ramp
T-2C	Half	10,000	38	50	23	34	85	77
		11,800	30	34	20	35	90	89
	Full	10,000	48	52	24	40	84	67
		11,800	48	52	26	39	89	81
F-14A	MIL	48,000	36	36	35	39	102	103
		55,000	35	33	29	38	106	106
F/A-18A	MIL	32,800	51	51	44	51	111	105
		37,000	51	55	46	52	114	106
	MAX A/B	32,800	49	62	43	51	102	97
		37,000	61	66	40	54	114	106

substantial increase in acceleration experienced by the aircraft over the theoretical expectation. This results from a dynamic interaction between the landing gear and ski-jump ramp in which gear compression while traversing the ramp causes an "equivalent" shorter radius of curvature to be experienced by the aircraft, thus causing the higher acceleration.

The ability to predict the performance associated with the ski-jump-assisted takeoff using pilot-in-the-loop simulation is summarized in Table 3. This table contains the minimum takeoff airspeed achieved in flight test in comparison with the predictions for the T-2C, F-14A, and F/A-18A at all conditions tested for the 6- and 9-deg ramps. With the exception of the F-14A, which was limited to flight test speeds in excess of 100 knots, excellent correlation is indicated for all conditions tested.

Table 4 summarizes the ski-jump performance obtained in flight test for the T-2C, F-14A, and F/A-18A. The table compares the takeoff airspeed and ground roll for ski-jump and conventional field takeoff. It should be noted that minimum takeoff speed is defined by zero minimum rate of climb for the T-2C and F/A-18A; the F-14A minimums were limited by a 100-knot minimum speed restriction for single-engine flight safety. Table 5 presents the results in a "percent reduction" format. As shown in the table, takeoff distance reductions of up to 66% were demonstrated. Reduction in distance over a 50-ft obstacle is also shown in Table 5. The maximum reduction in distance over a 50-ft obstacle typically occurs at a takeoff speed greater than the minimum ski-jump takeoff speed. This is due to the considerable "flattening" of the trajectory at altitudes below 50 ft as the minimum ski-jump speed is approached. The reductions in distance are somewhat less than those achieved in ground roll but are still on the order of 35-55%. Takeoff speed corresponding to the maximum reduction in distance over a 50-ft obstacle is given in the last two columns of the table for reference.

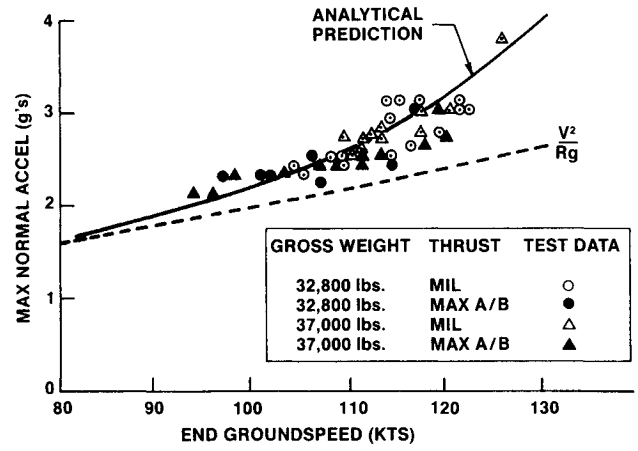

Fig. 12 F/A-18A ski-jump maximum normal acceleration 6-deg ramp (prediction vs flight test).

Conclusions

Through analysis, simulation, and flight test, the concept of ramp-assisted or ski-jump takeoff has been proved feasible for existing Navy aircraft. Analysis tools have been developed and have been proved, through flight test data correlation, to provide credible results for performance prediction purposes. The comparison of simulation and flight test results shows the analytical predictions of takeoff speed to be within 5% in all cases and, in general, conservative in nature. CTOL ski jump has been demonstrated to be practicable. The flight tests verified that performamce benefits are significant and warrant consideration for future fleet use. The success of the ski-jump feasibility demonstration with the T-2C, F-14A, and F/A-18A has led to a new initiative addressing the use of a small or

"mini" ramp in conjunction with existing stream catapults to enhance CTOL aircraft takeoff performance on current aircraft carriers. The ramp currently under study is approximately 42 ft long with an end angle of 2.15 deg and a maximum height of 14 in. This ramp, combined with a catapult, has the potential to reduce wind-over-deck (WOD) requirements for the F/A-18A by as much as 25 knots. Conversely, at the same WOD, the allowable takeoff gross weight could be increased by approximately 6000 lb.

Acknowledgments

The authors would like to acknowledge the contributions of the personnel of the Naval Aircraft Engineering Center, Lakehurst, New Jersey, and the Carrier Suitability Branch of the Naval Air Test Center, Patuxent River, Maryland, to the overall program described in this paper. The authors would also like to acknowledge simulation personnel at the NASA Ames Research Center, McDonnell Aircraft Company, and Naval Training Equipment Center for their support during piloted simulation efforts.

References

[1]Clark, J. W. Jr., "CTOL Ski Jump Feasibility: Technical Overview and Simulation Results," *Proceedings of the 1981 Air Force/Navy Science & Engineering Symposium*, Dayton, OH, Vol. 3: Flight Vehicles, 1981, pp. 399-434.

[2]Smith, A. A. et al., "Initial Conventional Takeoff and Landing (CTOL) Ski Jump Evaluation," NAVAIRTESTCEN Rept. SA-74R-80, Oct. 1980.

[3]Senn, C. P., "Conventional Take-off and Landing (CTOL) Airplane Ski Jump Evaluation," *Proceedings of the 15th Annual Society of Flight Test Engineerings Symposium*, St. Louis, MO, Aug. 1984.

[4]Senn, C. P. et al., "First Interim Report: Conventional Take-off and Landing (CTOL) Aircraft Ski Jump Evalutation," NAVAIRTESTCEN Rept. SA-74A-83, Dec. 1983.